ISSN: 0067-2904

Hydrochemistry of Tigris River in Baghdad city, Iraq

Haneen Zaid Abdulazeez[1*], Ayser Mohammed Al-Shamma'a [1], Qays Jasim Saud[2]
[1]Department of Geology, College of Science, University of Baghdad, Baghdad, Iraq
[2] Ministry of industry and minerals, Iraq Geological Survey

Received: 4/12/2019 Accepted: 12/4/2020

Abstract

The main objective of this study was to investigate the current water-quality conditions in Tigris River, Baghdad, Iraq, and to determine how those conditions are changing over time of pollution, if any. A series of hydrochemical tests were carried out to ascertain the influence of major Cations and Anions, Total Dissolved Solids (TDS), Electrical Conductivity (EC) and Potential of hydrogen (pH) on the quality of water. Water samples (n=34) were collected along Tigris River from north to south Baghdad City; 17 on January 2019 and 17 on April 2019. The results of the tests were compared with the World Health Organization standards, and showed that all the ions in addition to EC and TDS are within the acceptable limits, except for the samples 7 and 16 where Sulfate concentration was above the acceptable limits. Therefore, the Tigris River water in most of the study area is acceptable for all kinds of consumption. The most common water type in the area was Ca Na Mg- SO_4 Cl HCO_3 in January 2019 and Na Ca Mg- SO_4 Cl in April 2019.

Keywords: Hydrochemistry- Baghdad- pollution- Tigris

هيدروكيميائية نهر دجلة في مدينة بغداد، العراق

حنين زيد عبد العزيز[1]، ايسر محمد الشماع [1]، قيس جاسم سعود[2]
[1]جامعة بغداد, كاية العلوم, قسم علم الارض ، كلية العلوم، جامعة بغداد، بغداد، العراق
[2]وزارة الصناعة و التعدين, هيئة المسح الجيولجي العراقية ، بغداد، العراق

الخلاصه

ان الهدف الأساسي من هذه الدراسة هو تقييم نوعية المياه في نهر دجلة في مدينة بغداد، العراق وتحديد كيفية تغير نوعيتها وتلوثها من بعض الملوثات الشائعة والواسعة الانتشار ان وجدت. أجريت سلسلة من الفحوصات المختبرية لمعرفة تأثير تراكيز الايونات الموجبة والسالبة، و مجموع الاملاح الذائبة و التوصيلية الكهربائية و الرقم الهيدروجيني على نوعية المياه. تم جمع 34 عينة مياه من نهر دجلة في بغداد من شمالها الى جنوبها. تمت عملية جمع العينات في فترتين ولكل فترة 17 عينة، الاولى في شهر كانون الاول 2019 و الثانية في شهر نيسان 2019. تم تحليل الايونات الموجبة و السالبة بالاضافة الى التوصيلية الكهربائية و مجموع الاملاح الذائبة ولجميع النماذج، و مقارنة نتائج التحاليل مع معايير منظمة الصحة العالمية. و قد بينت نتائج التحاليل بأن جميع الايونات بالاضافة الى التوصيلية الكهربائية و مجموع الاملاح الذائبة هي من ضمن الحدود المسموح بها، ما عدا النموذجين رقم 7 و 16 حيث كان تركيز الكبريتات فيهما اعلى من الحد

*Email: alhaidaryhaneen@gmail.com

المسموح به، و لهذا فأن الماء في معظم منطقة الدراسة صالح للشرب. تصنيف و نوع المياه الاكثر شيوعا في منطقة الدراسة لشهر كانون الثاني صوديوم كالسيوم مغنيسيوم – كبريتيد كلور واما بالنسبة لشهر نيسان فقد كان التصنيف صوديوم مغنيسيوم – كبريتيد كلور الكربونات الثنائية.

Introduction

In Iraq, Tigris River and its tributaries are valuable resources that provide water necessary for drinking for an increasing population, crops irrigation, and habitats for aquatic life, in addition to its remarkable recreational opportunities .

Tigris, along with Euphrates, makes up a river system that borders Mesopotamia in the area known as the Fertile Crescent. According to National Geographic, The Tigris River is one of the most important waterways in the Fertile Crescent and has supported cities in both Turkey and Iraq, including Hasankeyf, Mosul, and Baghdad, for centuries [1].

Tigris length is about 1800 km, of which about 400 km run through Turkey before entering Syria then Iraq. The total length of Tigris in Iraq is about 1418 km, which is more than three quarters of the total length, with 60 km in Baghdad. Yet, pollution from urban and agricultural areas continues to pose a threat to Iraq water quality. According to Briggs, many environmental changes have been occurring globally at rates that were never experienced before in our planet's recent history [2]. Since 1980, Iraq and its people have extremely suffered as a result of the continuing wars that have led to the almost total destruction of its infrastructure. This includes the destruction of oil refineries in addition to the burning of large numbers of oil wells along with leaking that constantly happens in oil pipelines which transfer crude oil and its derivatives (Figures-(1&2). In addition, water treatment plants have been destroyed in most of Iraq's cities, including Baghdad. As a result, millions of liters of sewage are directly discharged without any treatment to the rivers and their tributaries or groundwater reservoirs. Not only that, but also most of the sewage outlets of many service institutions, such as hospitals, power plants, oil refineries and others, which are located on the shoulders of rivers, have been discharging all their solid and liquid waste directly into the rivers, including the Tigris. Another factor is the recent flooding that washed pollutants from soil into rivers (Figure-3). As a result of all of the above, the Iraqi environment in general suffers from pollution that causes high risks both to the environment itself and to its inhabiting forms of life. The quality of water depends on the dissolved ions or other contaminants occurring in the water. Thus, this study attempts to evaluate the environmental pollution in the study area by collecting water samples from Tigris River in Baghdad and analyze them in the laboratories to detect any contamination. The study results presented here may assist in understanding the potential influence of the contaminants on designing a more cost-effective remediation plan for contaminated water. Some of the previous studies conducted on this area include a hydrogeological environmental assessment study by Ali [3], of the effects of Al- Rasheed electrical power plant on the quality of Tigris River, Southern of Baghdad using Canadian Water Quality Index (CCME WQI) by*Alazawii, et al.* [4], and assessment of magnetite polishing using Tigris River stream sediments in Baghdad by Awadh and Khalid[5].

Figure 1-Tigris River, Baiji City, Iraq.

A: Apr 17, 2014

B: October 6, 2018

Figure 2-Dug channel used to smuggle crude oil from Allas oil field, Tikrit Governorate [6]

Figure 3-Flooding in Dyala River, Dyala City, Iraq

The main aim of this study is to evaluate the water quality in Tigris River in Baghdad, where many facilities discharge waste directly into the river.

Location of the study area

Baghdad is the capital and the largest city in Iraq, the second largest city in the Arab world after the capital of Egypt, Cairo, and the second largest city in Western Asia, after Tehran city, Iran. According to Encyclopedia Britannica Online, the area of Baghdad is 204.2 km^2 and its population is more than 8 million which, however, is not based on official records [7]. The Tigris River passes from the middle of Baghdad, where the western side of the river is called Al Karkh area, while the eastern side is Al Rusafa. Moreover, Baghdad was the largest city of the middle Ages for much of the Abbasid era, peaking at a population of more than a million [8]. The study area covers 17 sampling stations along Tigris River flowing through Baghdad, within the following geographical coordinates: Longitude: 44◦18'10.455"- 44◦34'08.857"E and Latitude: 33◦27'46.232"- 33◦08'18.225"N (Figure-4).

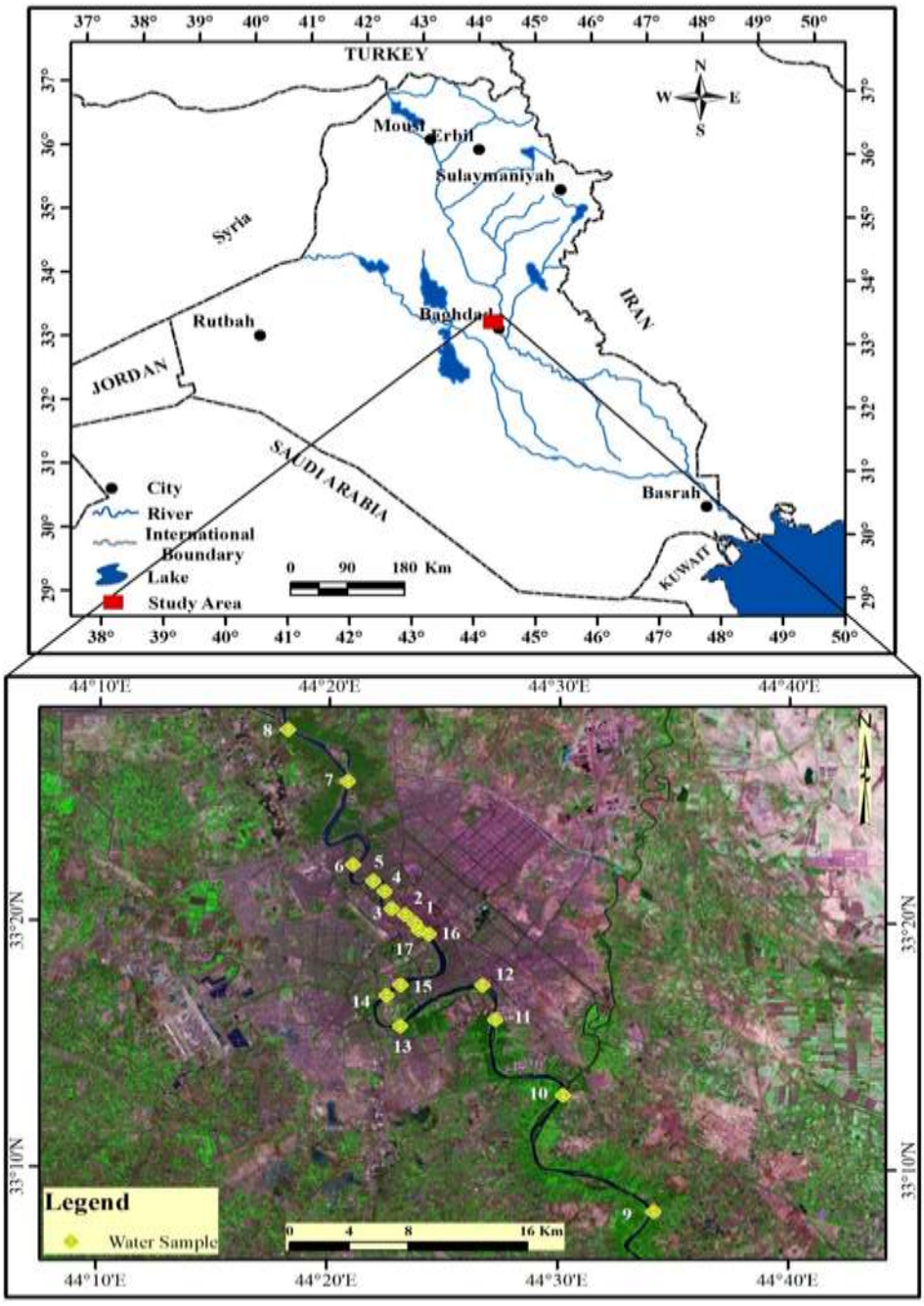

Figure 4- Location of the study area.

Table 1- Location of the collected samples

Station No.	Site names	Coordinates	
		N	E
1	**Al- Ahrar bridge**	33˚19'58.148"	44˚23'45.333"
2	**Al-Shuhada'a bridge**	33˚ 20'17.99"	44˚23'18.474"
3	**Bab AL-Muazm bridge**	33◦20'32.416"	44◦22'44.252"

4	**Al-Sarafia bridge**	33◦21'13.797"	44◦22'25.312"
5	**AL-A'azamia bridge**	33◦21'39.286"	44◦21'54.955"
6	**Al-A'ema bridge**	33◦22'19.363"	44◦21'02.245"
7	**Al- Muthana bridge**	33◦25'42.286"	44◦20'47.481"
8	**Tigris arm canal**	33◦27'46.232"	44◦18'10.455"
9	**Salman pack**	33◦08'18.225"	44◦34'08.857"
10	**Al – Tuaetha**	33◦13'00.00"	44◦30'12.579"
11	**Al- saeeda**	33◦16'03.322"	44◦27'16.484"
12	**Al-Rasheed oil station**	33◦17'26.556"	44◦26'42.745"
13	**AL- Dora electricity station**	33◦15'46.413"	44◦23'07.376"
14	**AL- Jadyrea bridge**	33◦17'00.619"	44◦22'31.913"
15	**Suspended bridge**	33◦17'27.026"	44◦23'0.8147"
16	**AL- Jumhuria bridge**	33◦19'31.874"	44◦24'21.277"
17	**AL- Senk bridge**	33◦19'41.297"	44◦23'55.902"

Geological setting

According to Jassim and Goff, the study area lies within the Stable shelf in the Mesopotamian zone, which contains the Tigris River and is covered with Quaternary sediments which overlie a complete Mesozoic and Cenozoic section [9]. The Quaternary sediments include Pleistocene and Holocene sediments. Geologic formations that crop out in the study area are the Pleistocene sediments which comprise Al-Fat'ha alluvial fan sediments, terrace of Euphrates River, gypcrete, and old flood plain sediments, as shown in Figure-5. The Holocene sediments comprise the flood plain; valley and depression fill sediments, marsh sediments, aeolian sediments and Anthropogene sediments (according to Deikran and Yacoub). The Fat'ha (Lower Fars) Formation is of the Middle Miocene age; its lower part is composed of alternating thick greenish and reddish silty claystone with layers of thinly bedded limestone and grayish sandstone. The upper part is composed of alternating beds of anhydrite, gypsum and salt, inter-bedded with limestone, marl, and relatively fine grained clastic, as shown in Figure-5. Gypcrete (Pleistocene) is intensively developed in the area between the Euphrates River and Al-Razzaza Lake, covering the sediments of Injana Formation and the remnants of the terrace sediments. Gypcrete, in the map, has a thickness range of 0.5 – 2 m. Undifferentiated Pleistocene Sediments, boreholes that penetrated the fluvial sediments below the flood plain sediments in the Mesopotamia Plain, are of the Pleistocene age and stratigraphically equivalent to the exposed Euphrates terrace sediments and alluvial fan sediments of the Tigris River. These fluvial sediments consist mainly of sand, pebbly sand and sandy gravels. The gravels gradually decrease east and southeastwards, towards the axis of the quaternary fluvial basin, with a total thickness of about 30 m in the area between Tigris and river. However, the thickness is expected to be greater further towards off the basin [10].

According to Deikran and Yacoub, the Flood plain sediments represent the most extensive sediments in the map area, which are the main Holocene sedimentary cycle of the Mesopotamia basin. Three rivers, namely Euphrates, Tigris, and Diyala-partly from Al-Udhaim River- were mainly the source of deposition of the flood plain. Each river develops district flood plain starting from the river channel, through natural levee to the flood basin. These morphologic elements of the flood plain have deposited with characteristic sedimentary facies. They differ from each other by grain size distribution and sedimentary structures. The valley filling sediments are mainly concentrated on the alluvial fan and terrace sediments, whereas in the Mesopotamia flood plain district, they are rare. The valleys are generally wide and shallow; some of them pass to wide depression. They are filled by fine Clastic rocks where clayey silt, silty-clay, and mud are dominating, with few admixtures of fine pebbles and rock fragments that contain very fine gypsum grains or powdered gypsum. Also, they are contaminated by windblown materials. Marsh sediments are developed in some depressions, which are characterized by distinct organic mud horizon with dark grey or black color, deposited to soil, indicating dense humiliated plants [11].

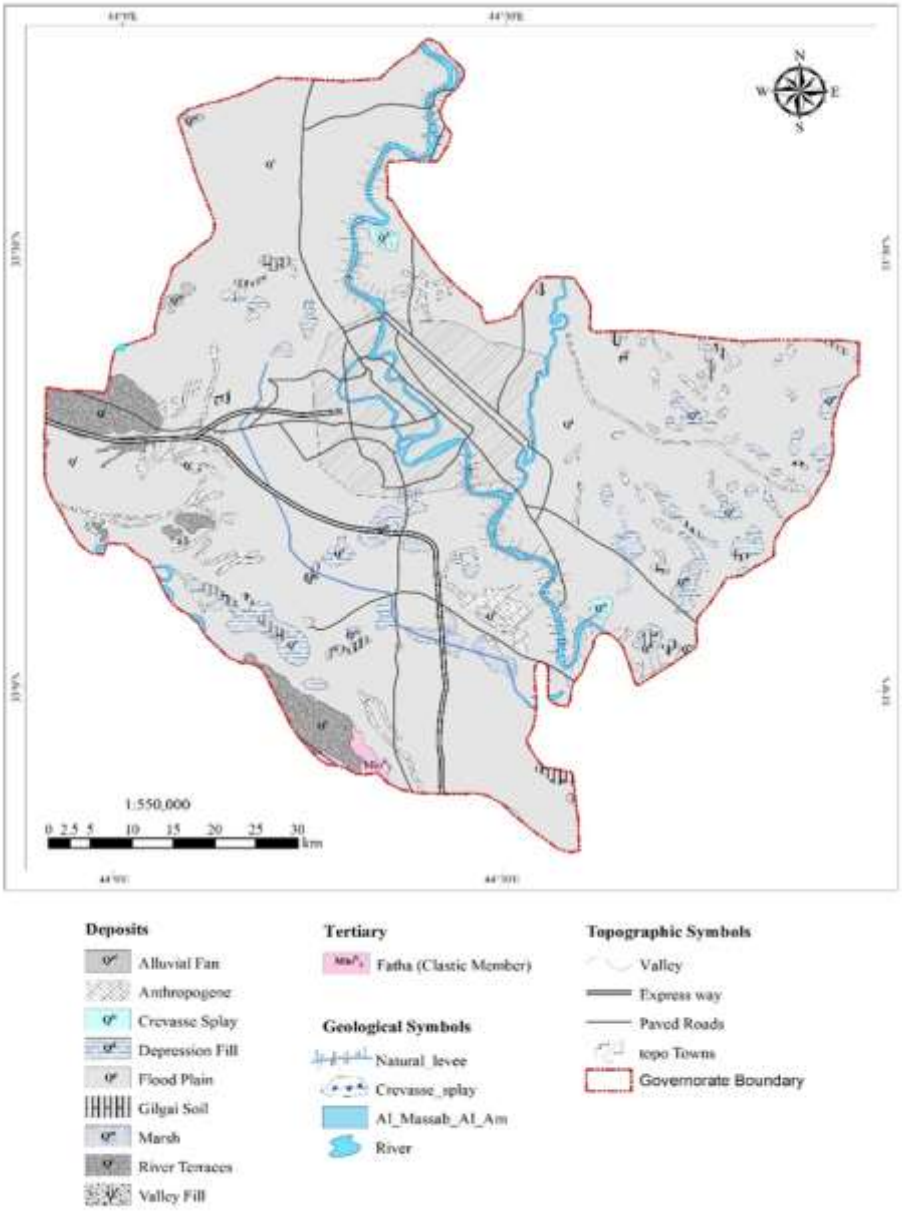

Figure 5-Geological map of Baghdad [11].

Materials and methods

Preliminary office work included gathering all available related literatures, theses, and researches that correspond with geology, hydrology and hydrogeological information of the study area. Moreover, topographic, geological maps were prepared, while climate data were collected from Baghdad meteorological station for the period 1996-2016.

Thirty four water samples were collected from different locations of Tigris River to cover the study reach of the river within two periods; January and April of 2019.

Locations of the samples were marked on the map by using GIS software (Figure-5). Each water sample was placed in a plastic bottle of 500 mL volume, with screw-on lid, where two samples were collected for each sample point; the first one for analyzing the major components, and the second for heavy metals analyses. All water samples were immediately covered with a tight screw-on lid, and perfectly labeled. No free headspace was left in the plastic bottle and it was ensured that the water sample in each bottle was in contact only with the plastic screw cap and plastic of the bottle. Table-3 illustrates the devices that were used during sampling procedure. WHO Guidelines of drinking water were compared to the ions concentration of water samples to find out if the water in the study area is suitable for human consumption or not.

Physical and chemical analyses of water samples were performed for the parameters of major ions (cations and anions), which are (Potassium (K^+), Sodium (Na^+), Cadmium (Ca^{+2}), Magnesium (Mg^{+2}), chloride (Cl^-), Sulfate (SO_4^{-2}), and Bicarbonate (HCO^{3-}), as well as minor ions, which are nitrate (NO^{3-}) and Phosphate (PO_4^{-3}), along of the parameters of pH, temperature, total dissolved solids (TDS), electrical conductivity (EC), total hardness (T.H.).

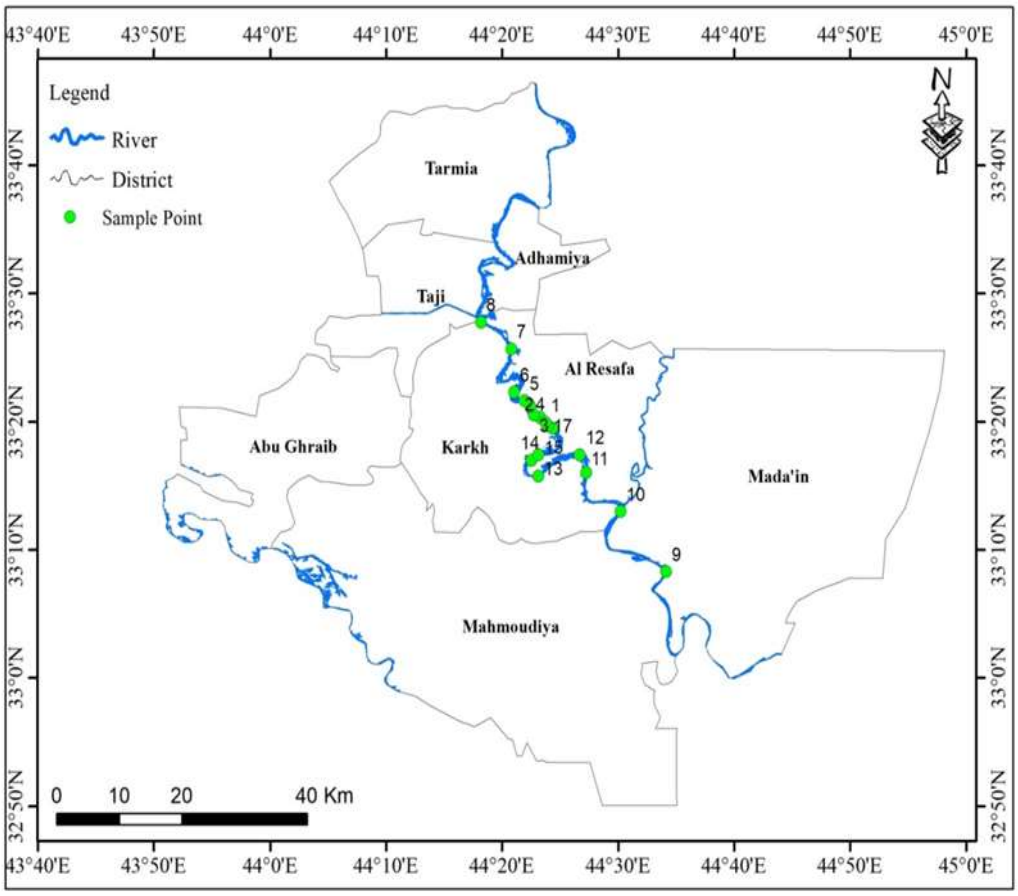

Figure 6-Sampling site location map.

Table 2- Equipment used for sampling.

E**quipment**	**Purpose**
Global Positioning System (GPS)	To pinpoint geographic location of all samples
Electrical conductivity meter (EC meter)	Measure an electrical conductivity of water samples
Thermometer	For measuring and indicating water samples temperature (°C)
Potential of hydrogen (pH meter)	A measure of acidity or alkalinity of water-soluble substances

In order to find the accuracy of the laboratory test the following equations were used:

$$(R\ D)\% = rC - rA / rC + rAx\ 100 \quad \ldots\ldots\ldots\ldots (1)$$

where:
R D = Relative Difference
rC = summation of cations in epm units.
rA =summation of anions in epm units.

$$A\% = 100 - R.D\ \% \quad \ldots\ldots\ldots\ldots\ldots\ldots\ldots\ldots (2)$$

where:
A% = Accuracy
According to Stoodly, the results could be accepted for interpretation when A ≥ 95%, and less accuracy would be acceptable with risk, but if the value is less than 90 % then it is not accepted for interpretation [12]. For further insurance, a sample was duplicated in each test to increase the precision of the tests. According to Maxwell, precision represents the degree to which the repeated measurements show the same results. Therefore, the next equation was used [13]:

$$P = 2S / x \times 100 \quad \text{----------} (3)$$

where:
P = precision with level of confidence at 95 %
S = standard deviation
x = arithmetic mean

According to Al-Janabi *et al*. the maximum acceptable limit for p is ± 20% [14].

To classify water and determine its type, two methods were used; the first is the hydrochemical (Kurolov) formula and the second is Piper diagram. The hydrochemical formula depends on the ratio of the main cations and anions, expressed as epm %, that are arranged in a descending order and have more than 15% ratio of availability, according to Ivanov*et al*. The cations are usually located at the base while the anions are located above. In addition, TDS (mg/L) and pH values as in the following formula:

Anions epm% decreasing order
TDS mg / L ——————————————— pH [15]
Cations epm% decreasing order

Piper diagrams, according to Fetter, allow both the anions and the cation to be represented on a single graph. These diagrams are also useful for visually describing the differences in major ions chemistry in water flow systems [16]. Piper diagram can be divided into seven types of water [17].

Results and Discussion

The climate data from Baghdad meteorological station for the period 1996-2016 are listed in Table-3.

Table 3- Climatic data for Baghdad Meteorological Station (1996 – 2016)

Month	Rainfall (mm)	Mean temperature (°C)		Evaporation (mm)	Relative Humidity (%)	Wind Speed (m/sec)	Sunshine (h/day)
		Max.	Min.				
Oct.	8.68	25.31	17	423.1	41.22	2.69	8
Nov.	22.76	16.8	10.15	195.36	59.33	2.34	6.99
Dec.	16.46	12	6.16	142.06	66.56	2.49	5.99
Jan.	22.97	10.05	4.67	66.27	68.22	2.61	6.14
Feb.	12.8	13.06	6.62	188.16	57.5	2.84	7.2
Mar.	13.72	17.62	10.61	336.61	45.83	3.19	7.77
Apr.	13.2	23.59	15.95	470.65	38.78	3.22	8.67
May.	3.92	29.68	21.45	666.87	30.78	3.22	9.81
Jun.	0	33.54	24.45	892.75	24.39	3.87	11.60
Jul.	0	36.06	24.87	976.33	23.78	3.88	11.53
Aug.	0	35.63	27.02	878.65	25.17	3.32	11.35
Sep.	0.12	31.24	26.56	651.59	30.94	2.94	9.99
Annual mean	114.63	23.71	16.29	490.7	42.7	3.05	105.04

All the water samples have an acceptable accuracy as shown in Tables- (4, 5), and the precision of the tests of TDS and EC are also acceptable. Therefore, the result of the laboratory tests listed in Tables-(6, 7) can be used for interpretation.

Table 4-Accuracy of chemical analysis of January 2019 samples

Sample number	RD %	Accuracy
1	0.83	99.17
2	1.21	98.79
3	0.51	99.49
4	0.84	99.16
5	1.00	99.00
6	0.23	99.77
7	0.54	99.46
8	0.22	99.78
9	1.67	98.33
10	0.25	99.75
11	0.92	99.08
12	0.31	99.69
13	1.45	98.55
14	1.77	98.23
15	0.05	99.95
16	0.88	99.12
17	0.95	99.05
18	0.97	99.03

Table 5-Accuracy of chemical analysis of April 2019 samples

Sample number	RD %	Accuracy
1	2.07	97.93
2	0.85	99.15
3	1.17	98.83
4	2.24	97.76
5	1.54	98.46
6	1.00	99.00
7	0.86	99.14
8	-0.03	100.03
9	0.08	99.92
10	0.66	99.34
11	4.53	95.47
12	3.66	96.34
13	1.50	98.50
14	5.18	94.82
15	1.26	98.74
16	2.99	97.01
17	3.68	96.32
18	1.83	98.17

Table 6-Concentration of major elements in water samples of January 2019

Sample No.	Cations				Anions			TDS	EC
	Ca^{2+}	Mg^{2+}	Na^{+}	K^{+}	Cl^{-}	SO_4^{-2}	HCO_3^{-}		
	(ppm)								(µS/cm)
1	58	23	49	0.6	95	146	67.50	438	876
2	61	24	51	0.7	93	152	77.98	460	919
3	65	23	50	0.9	95	150	87.98	472	944
4	58	21	53	0.6	93	151	64.08	440	881
5	57	22	51	2.8	92	148	67.98	441	881
6	59	23	50	2.4	93	150	77.98	455	910
7	56	17	63	0.5	80	159	78.67	453	906
8	59	19	70	0.4	74	166	120.00	508	1015
9	55	18	66	0.4	77	163	87.98	467	933
10	42	25	64	0.4	83	163	68.99	446	891
11	63	25	56	3.3	102	157	86.31	493	985
12	67	26	57	0.3	125	156	68.25	500	999
13	64	28	51	0.3	106	161	68.59	479	958
14	74	24	56	0.7	96	154	116.35	521	1043
15	66	25	55	1.6	69	153	160.00	530	1059
16	62	26	65	2.0	101	162	108.99	528	1055
17	66	26	56	3.3	81	154	140.81	527	1055
18	68	26	56	2.3	63	134	201.01	550	1100
WHO (2018)	**200**	**150**	**100**	**12**	**250**	**250**	**-**	**1000**	**-**

Table 7-Concentration of major elements in water samples of April 2019

Sample No.	Cations				Anions			TDS	EC
	Ca^{2+}	Mg^{2+}	Na^{+}	K^{+}	Cl^{-}	SO_4^{-2}	HCO_3^{-}		
	(ppm)								(µS/cm)
1	62	37	72	5	144	225	30	610	886
2	58	34	65	3.6	136	192	26	593	878
3	59	34	64	3.5	135	193	25	592	878
4	63	38	74	6	147	228	32	615	888
5	55	32	60	2	131	193	24	575	870
6	57	33	64	3.4	135	190	25	584	876
7	75	42	82	8	170	259	48	730	1065
8	63	37	73	5.5	145	227	32	616	888
9	45	24	70	4	131	137	18	460	693
10	40	20	60	2.1	106	129	16	400	596
11	67	40	80	7	156	240	36	640	906
12	66	40	78	7	155	238	35	638	905
13	76	46	89	7.8	165	250	39	674	918
14	72	43	84	7.5	160	244	37	660	912
15	75	45	87	7.7	164	249	38	675	916
16	80	48	96	11	188	288	57	772	1101
17	52	30	85	1.2	195	140	22	570	863
18	58	33	64	3.4	135	190	25	585	876
WHO (2018)	**200**	**150**	**100**	**12**	**250**	**250**	**-**	**1000**	**-**

Water classification

The classification of water samples using hydrochemical formula concluded that there are three water types, ordered from more to less common, in each period, as follows:

For January 1- Ca Na Mg- SO_4 Cl HCO_3

2- Na Ca Mg- SO_4 Cl HCO_3

3- Ca Na Mg- SO_4 HCO_3 Cl

4- Ca Na Mg- SO_4 Cl

And for April: 1- Na Ca Mg- SO_4 Cl

2- Ca Na Mg- SO_4 Cl

3- Na Ca Mg- Cl SO_4

As for Piper diagrams, they showed that all the water samples fall in the field of alkaline earth, in which (Ca^{2+} and Mg^{2+} are dominant with increased Na^{+} and prevailing sulfate, as shown in Figures-(8,7).

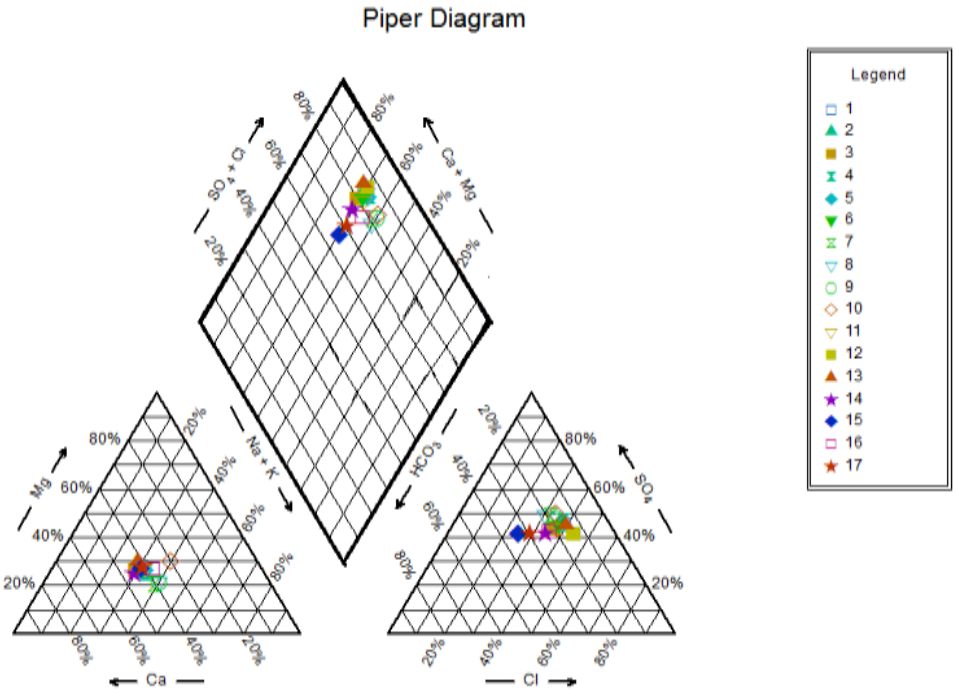

Figure 7-Piper diagram for water samples in January 2019.

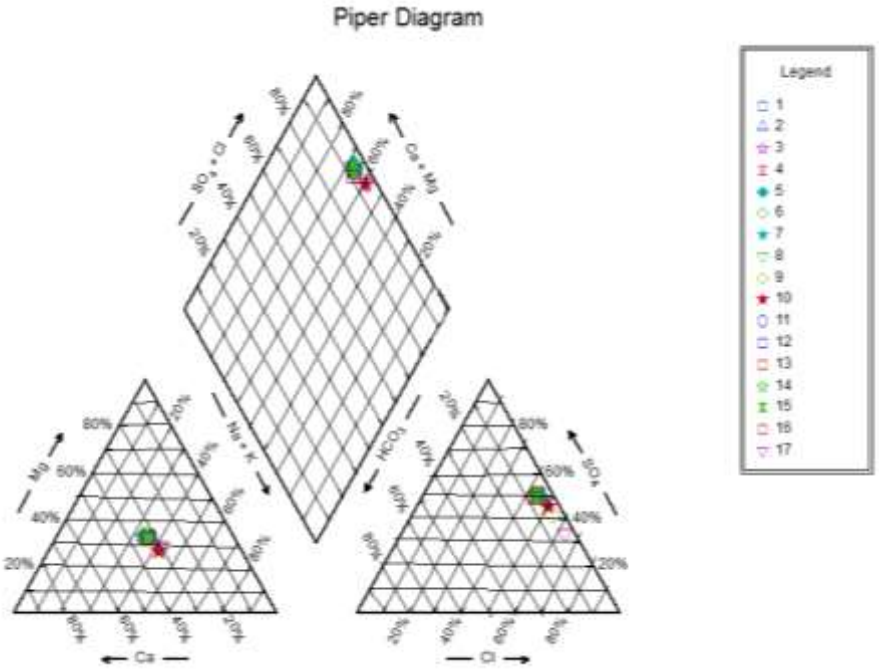

Figure 8-Piper diagram for water samples in April 2019.

The dominating Ca^{2+} and Mg^{2+} may cause water hardness and the high Na^{+} concentration may be due to domestic and factories waste, while the dominating SO_4 might be caused by scales build up on pipes and stains for clothes.

Conclusions

Based on the results of hydrochemical tests and WHO (2018) guidelines[18], it was found that:

1- TDS and EC values for all water samples are within the WHO limits of drinking water.

2- Calcium concentration in all samples was acceptable, with an average of 61.88 and a range between 40 to 80 ppm for both seasons.

3- Magnesium concentration was acceptable in all samples, and it ranged from 17 to 48 ppm with an

average of 32 ppm.

4- Sodium concentration in all samples was acceptable. with the average and it ranged between

5- Potassium concertation was acceptable in all samples and it ranged from 0.3 to 8 ppm with a mean of 4.15 ppm.

6- The concentrations of most ions in the second season were higher than those in the first season, which could be due to high rainfall rate with the resulting washing of chemical substances to the river from soil or storm drainage.

The most common water type in January 2019 was Ca Na Mg- SO_4 Cl HCO_3 while that in April Na Ca Mg- SO_4 Cl.

References

1. National Geographic**. 2019**. Tigris River. Available at https:// www. nationalgeographic.org /encyclopedia/tigris-river/ Access on 19 September, 2019.
2. Briggs, D., **2003**. Environmental pollution and the global burden of disease. *British Medical Bulletin*, **68**(1): 1–24, https://doi.org/10.1093/bmb/ldg019. Accessed on 14/07/18.
3. Ali S. M. **2012**. Hydrological environmental assessment of Baghdad area, Ph. D. Thesis, university of Baghdad.
4. Alazawii L. H., Nashaat M. R. and Muftin F. Sh. **2018**. Assessing the Effects of Al- Rasheed Electrical Power Plant on the Quality of Tigris River, Southern of Baghdad by Canadian Water Quality Index (CCME WQI). *Iraqi Journal of Science*, 2018, **59**(3A): 1162-1168.
5. Awadh S. M. and Khalid S. A. **2019**. Assessment of Magnetite Polishing by Using Tigris River Stream Sediments in Baghdad: An Ore Microscopy Application. *Iraqi Journal of Science*, 2019, **60**(2): 330-340.
6. Saud, Q. J. **2014**. Effects of Selected Contaminants on the Physical, Chemical, and Geotechnical Properties of Aquifer Solid. Ph.D. Thesis, University of Missouri-Kansas City. Available at: https://hdl.handle.net/10355/45614. Access on 14 May 2019.
7. Encyclopædia Britannica Online**, 2011**. Baghdad. http://www.newworldencyclopedia.org/ entry/Baghdad#cite_note-largestcities-1 Accesses on April 2019.
8. Thoughtco, Co**. 2011**. Largest Cities through History Geography. Accesses on April 2019. https://www.thoughtco.com/largest-cities-throughout-history-4068071
9. Jassim, S. Z. and Goff, J. C**. 2006.** Geology of Iraq, Published by Dolin, Pragh and Moravian Mueseum, Brno, p. 302
10. Deikran, D.B. and Yacoub, S.Y. **1993.** Series of geological maps of Iraq scale 1:250000, Baghdad Quadrangle (NI-38-10). GEOSURV, int. rep. no. 2255.
11. Sissakian, V.K. and Fouad, S.F. **2016**. Geological Map of Iraq, 4th edit. Scale 1:1000000. Iraq Geological Survey, GEOSURV, Baghdad, Iraq.
12. Stoodly, K.D., Lewis, T. and Stantion, C.L. **1980**. *Applied Statistical Techniques*, John Wiley and Sons, London.
13. Maxwell, J. A. **1968**. *Rock and Minerals Analysis*, John Wiley and Sons, NewYork, p. 584
14. Al-Janabi, A.Y., Al-Saadi, N. A., Zainal, Y. M., Al- Bassam, K. S. and Al-Delaimy, M. R. **1992**. Work procedures of the S. E of Geological Survey and Mining, State Establishment of Geological Survey and Mining (GEOSURV), part 21, No. 2002.
15. Ivanov V. V. **1968.** The main genetic type of the Earth crust mineral water and their distribution in USSR. Inter. Geol. Cong. Of 23rd sessions, *Czechoslovakia*, **12**, 33p.
16. Fetter C.W**. 2001**. *Applied Hydrogeology*, (3rded.). Prentice Hall, Inc., Englewood Cliffs, New Jersey, 691p.
17. Piper, A. M. **1944**; A graphic procedures in geochemical interpretation of water analysis. Trans. Am. *Geophys. Union*, **25**: 914 – 923.
18. WHO (world health organization), **2018**. A global overview of national regulations and standards for drinking-water quality. Licence: CC BY-NC-SA 3.0 IGO. Available at: http://apps.who.int/iris/bitstream/handle/10665/272345/9789241513760-eng.pdf?ua=1 Access on 14 July 2.